

Stability and Transient Performance Assessment in a COTS-Module-Based Distributed DC/DC System

S. Vesti, J.A. Oliver, R. Prieto, J.A. Cobos
 Centro de Electrónica Industrial
 Universidad Politécnica de Madrid
 Madrid, Spain

T. Suntio
 Tampere University of Technology
 Tampere, Finland

Abstract—This paper introduces a method to analyze and predict stability and transient performance of a distributed system where COTS (Commercial-off-the-shelf) modules share an input filter. The presented procedure is based on the measured data from the input and output terminals of the power modules. The required information for the analysis is obtained by performing frequency response measurements for each converter. This attained data is utilized to compute special transfer functions, which partly determine the source and load interactions within the converters. The system level dynamic description is constructed based on the measured and computed transfer functions introducing cross-coupling mechanisms within the system. System stability can be studied based on the well-known impedance-related minor-loop gain at an arbitrary interface within the system.

I. INTRODUCTION

The use of distributed systems in processing electricity is growing fast in different applications areas such telecom, ship, avionic and automotive applications [1]–[6]. These systems can be very complicated consisting of various components, which are sensitive to interactions. The design of the main system component, high-frequency switched-mode converter is extremely demanding task especially as low cost and volume, high efficiency, reliability and short time-to-market are to be optimized. Therefore, the DC/DC system design is frequently based on the use of ready-made power supply modules [1]–[4] known as COTS (i.e., component of the self) to avoid the need of high-level specialists in the converter design.

The system design is often assumed straightforward and easy, merely adding the connections between the converters as well as additional EMI filtering if necessary. However, the impedance interactions between the converters and the passive filters can destroy the system stability and/or deteriorate the converter transient performance to be unacceptable if the interactions are not damped sufficiently [5], [7]–[14]. These interactions can be analyzed by representing the dynamics of a switched-mode converter by means of two-port network parameters i.e., a set of transfer functions known as G parameters for a voltage-input-voltage-output converter [15]–[18]. In case of ready-made power modules, only four measurable transfer functions exist. Thus it is obvious that the stability and transient performance analysis is required to be based on them.

The power system analysis is typically accomplished by dividing the system into smaller parts i.e. subsystems to facilitate the design and analysis. Within this paper a method to analyze and predict stability and transient performance of a specific system part is presented. This subsystem, consisting of two commercial converters with a common input filter, forms a part of a larger distributed power system as shown in Fig. 1, where the subsystem to be analyzed is emphasized. This distributed power system is designed for high reliability application and the commercial converters utilized within the system are selected based on the requirements set for the application field.

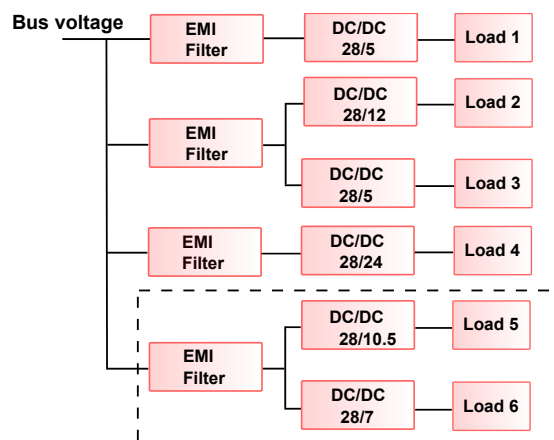


Fig. 1. Complete distributed power system, where the highlighted area illustrates the subsystem to be analyzed.

This paper provides theoretical formulation for the interactions analysis within the described system structure. The system stability can be determined at an arbitrary interface applying the impedance ratio known as minor-loop gain [14]. For more detailed interactions analysis, the DC/DC converters are first modeled utilizing an unterminated two-port model [19] where the source and load effects are excluded. Thereafter, by including the source impedance as a part of the system, the influence of the common input filter to the subsystem performance can be analyzed in detail. Correspondingly, the load-affected dynamic representation of the system is obtained by considering the load admittance as a part of the system.

The necessary data for the power module characterization

is obtained by performing frequency response measurements for the selected ready-made converters. Subsequent to this, the interactions and possible performance degradations can be analyzed based on the presented theoretical formulation. Thus the suitability of the selected converters for the intended application can be verified.

II. THEORETICAL APPROACH

The system interaction analysis is initiated by modeling a single DC/DC converter as two-port network that consists of a set of transfer functions, at open loop or closed loop. This is a unified model, applicable to any converter independent of the topology, operation or control mode and therefore, suitable also for modeling commercial converters. In case of ready-made converters, only four closed-loop transfer functions are obtainable according to (1).

$$\begin{bmatrix} \hat{i}_{in} \\ \hat{u}_o \end{bmatrix} = \begin{bmatrix} Y_{in} & T_{oi} \\ G_{io} & -Z_o \end{bmatrix} \cdot \begin{bmatrix} \hat{u}_{in} \\ \hat{i}_o \end{bmatrix} \quad (1)$$

These transfer functions are input admittance Y_{in} , reverse transfer function T_{oi} , audio susceptibility G_{io} and output impedance Z_{out} . Based on these G-parameters the converter can be presented as a two-port-network as illustrated in Fig. 2. Both, source and load are assumed to be ideal and, therefore, the highlighted area presents only the internal dynamics of the converter. Since the interactions are due to the converter dynamics, this modeling method enables detailed interactions analysis.

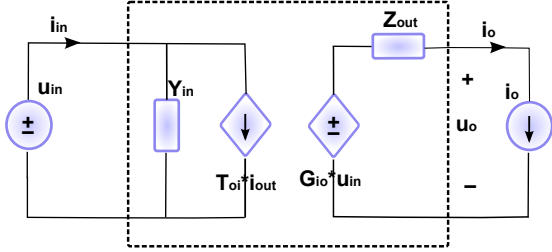


Fig. 2. Two-port-network model for a single DC/DC converter with ideal source and load.

A. Input parallel-connected converters

The described subsystem structure, input-parallel-connected converters with a common filter, is shown in Fig. 3. This system structure can be modeled as shown in Fig. 4 where both DC/DC converters are presented as their two-port networks. The corresponding internal dynamics of these input-parallel connected converters is given in (2).

$$\begin{bmatrix} \hat{i}_{in} \\ \hat{u}_{o1} \\ \hat{u}_{o2} \end{bmatrix} = \begin{bmatrix} Y_{in} & T_{oi1} & T_{oi2} \\ G_{io1} & -Z_{o1} & 0 \\ G_{io2} & 0 & -Z_{o2} \end{bmatrix} \cdot \begin{bmatrix} \hat{u}_{in} \\ \hat{i}_{o1} \\ \hat{i}_{o2} \end{bmatrix} \quad (2)$$

Within the dynamic representation of the system structure, the input filter is presented by source impedance Z_s and both loads by admittances Y_{L1} and Y_{L2} . The highlighted area

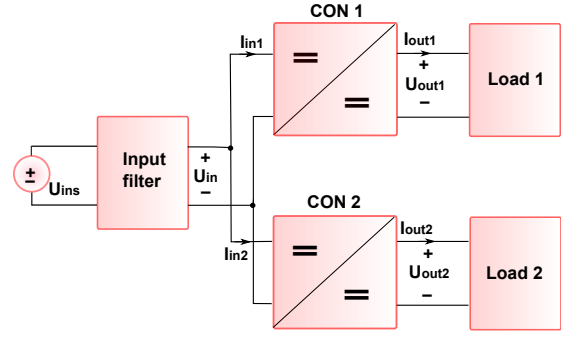


Fig. 3. Input-parallel connected subsystem with a common input filter.

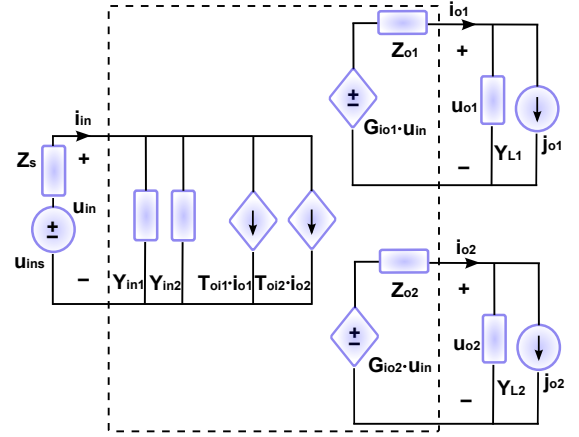


Fig. 4. Dynamic representation of the interconnected system.

shows the system to be analyzed i.e. input-parallel connected converters presented by their G-parameters.

B. Source-affected dynamic system

In order to analyze the source interactions, the input filter is included as a part of the system while the load is presented as an ideal current source. This system network model is shown in Fig. 5. The highlighted area illustrates again the system to be analyzed. However, as the source impedance is now included within the system, the converter G-parameters are considered as source-affected. Corresponding dynamical description is provided in (3), where the superscript 's' denotes source-affected. It can be seen that the common source impedance creates cross-couplings (i.e., $\hat{u}_{o1,2} / \hat{i}_{o2,1}$) between the converters. As a comparison to (2), where the cross-coupling transfer functions, $G_{cr1,2}$, are zero due to the ideal source, a load step at the other module output can influence on the output of the input-parallel-connected power module.

$$\begin{bmatrix} \hat{i}_{in} \\ \hat{u}_{o1} \\ \hat{u}_{o2} \end{bmatrix} = \begin{bmatrix} Y_{in}^s & T_{oi1}^s & T_{oi2}^s \\ G_{io1}^s & -Z_{o1}^s & G_{cr1}^s \\ G_{io2}^s & G_{cr2}^s & -Z_{o2}^s \end{bmatrix} \cdot \begin{bmatrix} \hat{u}_{ins} \\ \hat{i}_{o1} \\ \hat{i}_{o2} \end{bmatrix} \quad (3)$$

For detailed source influence definition, the whole system is solved again by replacing the ideal input voltage to the source-affected input. The obtained G-parameters are provided in (4).

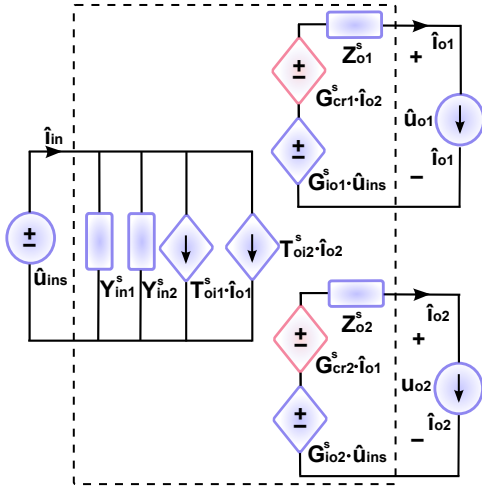


Fig. 5. Source-affected distributed system.

$$\begin{aligned}
 Y_{in}^s &= \frac{Y_{in}}{1 + Z_s Y_{in}} \\
 T_{oi1}^s &= \frac{T_{oi1}}{1 + Z_s Y_{in}} \\
 T_{oi2}^s &= \frac{T_{oi2}}{1 + Z_s Y_{in}} \\
 G_{io1}^s &= \frac{G_{io1}}{1 + Z_s Y_{in}} \\
 -Z_{o1}^s &= -\frac{1 + Z_s(Y_{in-sco1} + Y_{in2})}{1 + Z_s Y_{in}} Z_{o1} \\
 G_{cr1}^s &= -\frac{G_{io1} T_{oi2} Z_s}{1 + Z_s Y_{in}} \\
 G_{io2}^s &= \frac{G_{io2}}{1 + Z_s Y_{in}} \\
 G_{cr2}^s &= -\frac{G_{io2} T_{oi1} Z_s}{1 + Z_s Y_{in}} \\
 -Z_{o2}^s &= -\frac{1 + Z_s(Y_{in-sco2} + Y_{in1})}{1 + Z_s Y_{in}} Z_{o2}
 \end{aligned} \quad (4)$$

Where the system input admittance Y_{in} as well as the special parameters $Y_{in-sco1}$ and $Y_{in-sco2}$ for both converters are defined according to (5).

$$\begin{aligned}
 Y_{in} &= Y_{in1} + Y_{in2} \\
 Y_{in-sco1} &= Y_{in1} + \frac{G_{io1} T_{oi1}}{Z_{o1}} \\
 Y_{in-sco2} &= Y_{in2} + \frac{G_{io2} T_{oi2}}{Z_{o2}}
 \end{aligned} \quad (5)$$

These special parameters are known as short-circuit input admittances and they provide more insight on the source-affected interactions, regarding the source impedance influence on the converter output impedances. They are obtainable computationally from the measured transfer functions and can be defined for any converter either at open- or closed-loop. More detailed interpretation of these parameters is provided within the next section.

C. Load-affected dynamic system

Similarly, the load influence can be included to the presented system dynamics and its influence on the rest of the system can be analyzed. This is implemented by including the load admittance to the system as was illustrated in Fig. 4, and solving the corresponding equations considering the load as part of the system. The dynamical description as the influence of the module one load admittance Y_{L1} is regarded is given in (6) where the superscript 'L1' denotes load-affected.

$$\begin{bmatrix} \hat{i}_{in} \\ \hat{u}_{o1} \\ \hat{u}_{o2} \end{bmatrix} = \begin{bmatrix} Y_{in}^{L1} & T_{oi1}^{L1} & T_{oi2}^{L1} \\ G_{io1}^{L1} & -Z_{o1}^{L1} & G_{cr1}^{L1} \\ G_{io2}^{L1} & G_{cr2}^{L1} & -Z_{o2}^{L1} \end{bmatrix} \cdot \begin{bmatrix} \hat{u}_{ins} \\ \hat{i}_{o1} \\ \hat{i}_{o2} \end{bmatrix} \quad (6)$$

The source- and load-affected G-parameters are provided in (7) while the load admittance Y_{L1} considered as a part of the system.

$$\begin{aligned}
 Y_{in}^{L1} &= Y_{in}^s + \frac{Y_{L1} G_{io1}^s T_{oi1}^s}{1 + Z_{o1}^s Y_{L1}} \\
 T_{oi1}^{L1} &= \frac{T_{oi1}^s}{1 + Z_{o1}^s Y_{L1}} \\
 T_{oi2}^{L1} &= T_{oi2}^s + \frac{Y_{L1} G_{cr1}^s T_{oi1}^s}{1 + Z_{o1}^s Y_{L1}} \\
 G_{io1}^{L1} &= \frac{G_{io1}^s}{1 + Z_{o1}^s Y_{L1}} \\
 -Z_{o1}^{L1} &= -\frac{Z_{o1}^s}{1 + Z_{o1}^s Y_{L1}} \\
 G_{cr1}^{L1} &= \frac{G_{cr1}^s}{1 + Z_{o1}^s Y_{L1}} \\
 G_{io2}^{L1} &= G_{io2}^s - \frac{G_{io1}^s G_{cr2}^s Y_{L1}}{1 + Z_{o1}^s Y_{L1}} \\
 G_{cr2}^{L1} &= \frac{G_{cr2}^s}{1 + Z_{o1}^s Y_{L1}} \\
 -Z_{o2}^{L1} &= -(Z_{o2}^s - \frac{G_{cr1}^s G_{cr2}^s Y_{L1}}{1 + Z_{o1}^s Y_{L1}})
 \end{aligned} \quad (7)$$

Correspondingly, the system dynamics can be presented as in (8) and the G-parameters as given in (9), while the load admittance Y_{L2} is considered as a part of the system.

$$\begin{bmatrix} \hat{i}_{in} \\ \hat{u}_{o1} \\ \hat{u}_{o2} \end{bmatrix} = \begin{bmatrix} Y_{in}^{L2} & T_{oi1}^{L2} & T_{oi2}^{L2} \\ G_{io1}^{L2} & -Z_{o1}^{L2} & G_{cr1}^{L2} \\ G_{io2}^{L2} & G_{cr2}^{L2} & -Z_{o2}^{L2} \end{bmatrix} \cdot \begin{bmatrix} \hat{u}_{ins} \\ \hat{i}_{o1} \\ \hat{i}_{o2} \end{bmatrix} \quad (8)$$

Based on these equations, it is observable that the stability conditions as well as the transient performance of the other converter can be significantly changed from the original state due to the load impedance of the other input-parallel connected power module.

$$\begin{aligned}
Y_{in}^{L2} &= Y_{in}^s + \frac{Y_{L2}G_{io2}^sT_{oi2}^s}{1 + Z_{o2}^sY_{L2}} \\
T_{oi1}^{L2} &= T_{oi1}^s + \frac{Y_{L2}G_{cr2}^sT_{oi2}^s}{1 + Z_{o2}^sY_{L2}} \\
T_{oi2}^{L2} &= \frac{T_{oi2}^s}{1 + Z_{o2}^sY_{L2}} \\
G_{io1}^{L2} &= G_{io1}^s - \frac{G_{io2}^sG_{cr1}^sY_{L2}}{1 + Z_{o2}^sY_{L2}} \\
-Z_{o1}^{L2} &= -(Z_{o1}^s - \frac{G_{cr1}^sG_{cr2}^sY_{L2}}{1 + Z_{o2}^sY_{L2}}) \\
G_{cr1}^{L2} &= \frac{G_{cr1}^s}{1 + Z_{o2}^sY_{L2}} \\
G_{io2}^{L2} &= \frac{G_{io2}^s}{1 + Z_{o2}^sY_{L2}} \\
G_{cr2}^{L2} &= \frac{G_{cr2}^s}{1 + Z_{o2}^sY_{L2}} \\
-Z_{o2}^{L2} &= -\frac{Z_{o2}^s}{1 + Z_{o2}^sY_{L2}}
\end{aligned} \tag{9}$$

III. ANALYSIS

Subsequent to obtaining the theoretical formulation for the analysis of additional impedance influences on the presented system structure, the power modules need to be characterized. The required information for the presented dynamical representations is obtained by measuring four transfer functions from the input and output of both selected ready-made converters. This attained data is utilized to compute the special transfer functions $Y_{in-sco1}$ and $Y_{in-sco2}$ required for the source-affected interactions analysis.

A. Characterization

The commercial converters are selected based on the requirements set by the application area. They are from the same manufacturer and of same model, thus possessing equal topologies and control methods at the switching frequency of 500 kHz, with the following specifications:

- Module 1: $V_{out} = 12V$ and $I_{out} = 6A$
- Module 2: $V_{out} = 9.5V$ and $I_{out} = 6A$
- Input voltage range: 18V - 40V

Both converters are characterized by performing the frequency response measurements in order to obtain the relevant transfer functions for the described two-port model. The utilized measurement equipment was Venable Industries' frequency response analyzer Model 3120 with an impedance measurement kit. In order to maximize the input filter effects the frequency response measurements were performed at the minimum system input voltage at 18V.

The measured transfer functions for the module one are shown in Figs. 6, 7, 8 and 9 representing the audio susceptibility, input admittance, output impedance and reverse transfer function, respectively. It can be seen from Fig. 6 that the measured input-to-output attenuation G_{io} , is high, implying to a highly source invariant converter, preventing the interactions from propagating through the converter. From

Fig. 8 the output impedance can be observed to be small thus implying to a load invariant converter, that prevents the load-side interactions. Corresponding characterization is also performed for the second power module. The obtained characterization results are similar than the presented ones, since the only difference between the converters is the output voltage level.

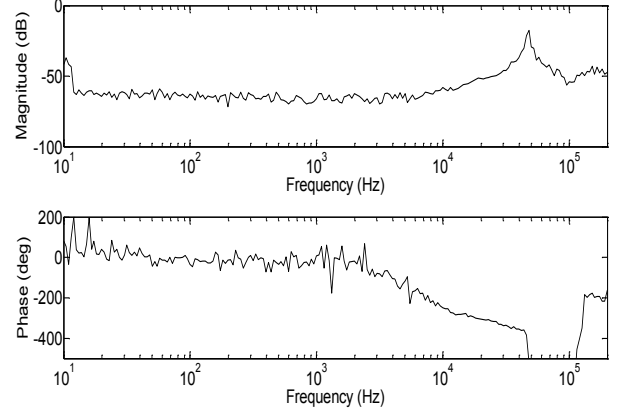


Fig. 6. Measured audio susceptibility G_{io} of the module one.

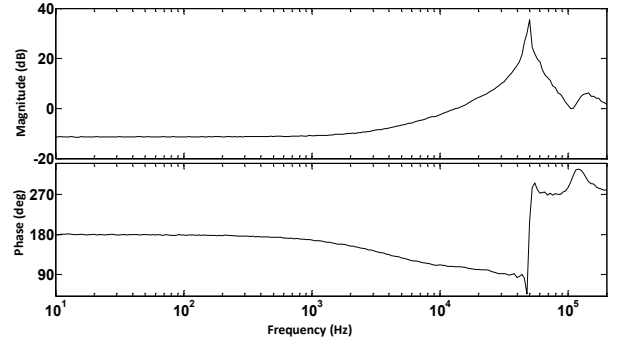


Fig. 7. Measured input admittance Y_{in} of the module one.

B. Interaction mechanism

The impedance interactions within the system are complex to analyze, especially in case of commercial converters when the available information regarding the converter dynamics is restricted. Even in the best case the data provided by the manufacturers is limited to the converter topology and utilized control method. This datasheet information, although useful for those who understand the dynamic behavior originating from different control methods, is still insufficient for analyzing and predicting the dynamic behavior of the interconnected system.

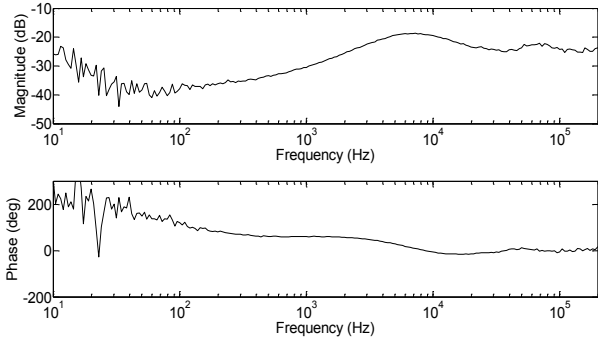


Fig. 8. Measured output impedance Z_o of the module one.

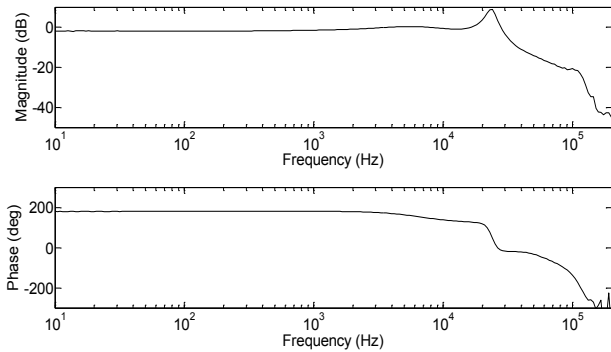


Fig. 9. Measured reverse transfer function T_{oi} of the module one.

The addition of the input filter, i.e. source impedance, can influence on the stability and/or the performance of the converters. These effects can be analyzed utilizing the extracted source-affected dynamic description of the system. Most relevant equation to be analyzed is the source-affected output impedance (10) that presents the input filter influence on the output impedance of converter one.

$$\begin{aligned} Z_{o1}^s &= \frac{1 + Z_s(Y_{in-sco1} + Y_{in2})}{1 + Z_s Y_{in}} Z_{o1} \\ &= \frac{1 + \frac{Z_s}{Z_{in-sco1}} + \frac{Z_s}{Z_{in2}}}{1 + \frac{Z_s}{Z_{in}}} Z_{o1} \end{aligned} \quad (10)$$

The compliance with the condition $Z_s \ll Z_{in}$ regarding the impedance inequality between filter output impedance and the system closed-loop input impedance determines the stability. This is a general and well-known input filter design rule. However, the fulfillment with this requirement does not necessary guarantee unaltered output impedance and transient response. Whereas, the compliance with the impedance in-

equality $Z_s \ll Z_{in-sco1}$ regarding the source impedance and the short-circuit input impedance provides a condition for the unaltered transient behavior.

The origin of the source-affected interactions can be analyzed in detail utilizing the defined special parameters, input short-circuit admittances $Y_{in-sco1,2}$ given in (5). Considering again the source-affected output impedance equation and by replacing the input short-circuit admittance $Y_{in-sco1}$ of converter one by its given definition, the output impedance of the module one can be expressed according to (11).

$$Z_{o1}^s = \frac{1 + Z_s(Y_{in1} + Y_{in2}) + Z_s \frac{G_{io1} T_{oi1}}{Z_{o1}}}{1 + Z_s Y_{in}} Z_{o1} \quad (11)$$

From the equation a term, $\frac{G_{io1} T_{oi1}}{Z_{o1}}$ consisting of the measured transfer functions that dependent on the applied control method and the conduction mode of the converter can be observed to contribute on the source-affected interactions.

The influence of different control methods and conduction modes to the input short-circuit impedance is demonstrated in [13] revealing that the voltage-mode-controlled buck converter is the most sensitive to these interactions whereas peak-current-mode-controlled buck converter exhibits reduced sensitivity to the input filter interactions. Therefore, the short-circuit input admittance is the most relevant parameter for a comprehensive source interactions analysis to determine whether the transient performance is deteriorated.

Depending on the system structure, the source-impedance influence on the converter output impedance varies. Within the described structure of input parallel-connected converters the source-affected output impedance is altered as a comparison to an individual converter and source impedance (See e.g. [12] [13]). In addition to directly influencing on the transient behavior of an individual converter, the common source impedance also introduces the cross-coupling mechanism within the system. Therefore, the transient behavior of the module two might be deteriorated while a load step is applied at the output of converter one.

By performing the described analysis procedures, the suitability of a commercial converter for a specific application can be evaluated. In case the input short-circuit impedance is observed to be smaller than the source impedance, the influences can be evaluated in detail based on the altered output impedance. Regarding the ready-made converters not many possibilities exist for solving the problem since the interactions are due to the inner dynamics of a specific DC/DC converter. Therefore, the possible options to guarantee unaltered system behavior are to replace the selected commercial converter, add capacitance at the filter output, or change the filter resonant frequency to higher frequencies. The effect of these optional actions can be evaluated by comparing the source impedance and the short-circuit input impedance ($Z_s \ll Z_{in-sco}$).

IV. DESIGN VALIDATION

The theoretical formulation describes how the dynamic representation of the source- and load-affected system is obtained

emphasizing the key equations regarding the source-affected interactions. Thereafter, as the power module characterization is performed, the design can be analyzed in detail based on the proposed approach to determine whether the selected converters are suitable for the described system structure.

The utilized components within the designed subsystem, including the EMI filter, are chosen based on the intended application field. Thus the most relevant requirements are high reliability and compliance with various authority requirements instead of low cost and volume. The manufacturer guarantees stable operation while multiple power module units are sharing the input filter up to the rated output current of the filter. The module characterization already alluded to reduced interactions, which could be also deduced based on the datasheet information. As the origin of the interactions has been proved to be dependent on the topology as well as the applied control method and mode of operation, the data sheet information implies that the selected power modules are buck-derived converters applying peak-current-mode control [20]. This control is proven to reduce the source-side interactions within the converter [21].

The possible source interactions are minimized provided that all the input-side admittances are equal. The output impedance remains unaltered subsequent the addition of the source impedance in case the input short-circuit admittance $Y_{in-sco1}$ of module one is equal to its measured input admittance Y_{in1} according to (12), where the system input admittance Y_{in} is expressed as a sum of the module input admittances.

$$Z_{o1}^s = \frac{1 + Z_s(Y_{in1} + Y_{in2})}{1 + Z_s(Y_{in1} + Y_{in2})} Z_{o1} \quad (12)$$

The design validation regarding the implemented system is performed by computing the short-circuit input admittances based on the measured transfer functions. Possible source interactions regarding the converter one are analyzed by comparing the input short-circuit admittance $Y_{in-sco1}$ and the measured closed-loop input admittance of the converter one as shown in Fig. 10.

Thus based on the comparison, the input admittances can be observed equal and, therefore, according to (12) it can be concluded that the source impedance does not alter the converter one output impedance. Correspondingly, the described analysis is performed in case of the other converter, providing the validation that the transient behavior remains unaltered.

As previously discussed, the load step introduced at the output of the converter one, might deteriorate the output voltage of the converter two due to the cross-coupling mechanism. The cross-coupling transfer function, obtained computationally or directly by measuring, is analyzed in order to determine possible interactions between the converters. Fig. 11 shows the computed and measured cross-coupling transfer function from the module one to the output of converter two. The cross-coupling impedance is attenuated thus indicating that module two output voltage remains invariant to the load transient applied at the output of converter one. This is confirmed within

time domain as shown in Fig. 12, where a load step from no load to full load is introduced at the output of the converter one. From the figure it is clearly seen that the output voltage U_{o2} remains unaffected.

Correspondingly, as the same analysis is performed for the other module, similar conclusions can be drawn. Therefore, subsystem characterization shows that the source impedance does not influence the performance of the converters and that the cross-couplings between the modules do not exist. Thus the converters work nicely as dynamic buffers preventing the interactions to be distributed within the system. The analysis proves the suitability of the selected converters for the intended high reliability application.

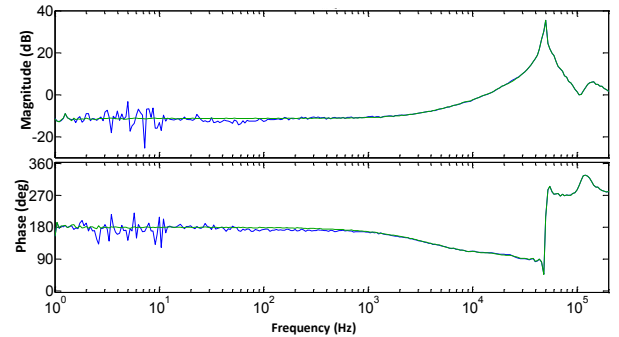


Fig. 10. Measured input admittance compared to the computed input short-circuit admittance, where green line presents the measured input admittance.

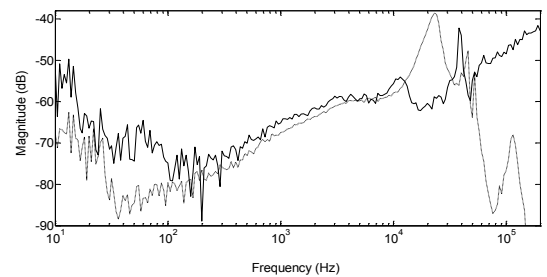


Fig. 11. Measured and computed cross-coupling impedance from the output of the module one to the output of module two, where the dashed line illustrates the computed parameter.

V. CONCLUSION

The main goal of the paper is to investigate the methods to characterize the ready-made power modules in such a way that the stability and transient performance of the overall

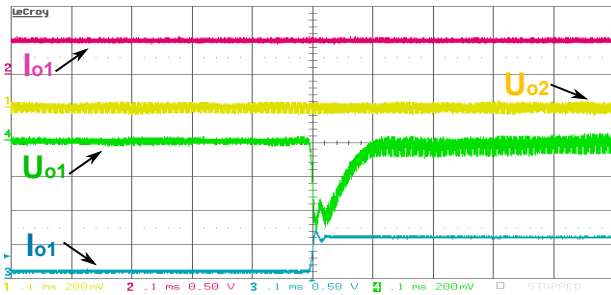


Fig. 12. A load step from no load to full load is introduced at the output of the module one.

distributed system can be assessed based on the measurable information through the input and output terminals of the associated converters. Theoretical approach on analyzing the system as the source and/or load impedance is included as a part of the described input-parallel connected system. Based on the presented procedure, possible interactions due to the common input filter can be analyzed in detail and determine whether the selected commercial converters are suitable for the intended application. Within the described system structure problems are most likely to occur in case the utilized converters are high-efficiency POL converters with voltage-mode control. In this paper a comprehensive characterization method of the commercial converters utilized within the described system, as well as the associated interactions are provided. It was demonstrated how the extracted information can be utilized within the presented system structure analysis and design. The created theoretical basis for the analysis of the described system structure were applied in practice for a subsystem of an existing system proving that the converters operate as dynamic buffers preventing the interactions to propagate within the system.

REFERENCES

- [1] M. P. Sayani and J. Wanes, "Analyzing and determining optimum on-board power architectures for 48 v-input systems," in *Proc. Eighteenth Annual IEEE Applied Power Electronics Conf. and Exposition APEC '03*, vol. 2, 2003, pp. 781–785.
- [2] M. Barry, "Design issues in regulated and unregulated intermediate bus converters," in *Proc. Nineteenth Annual IEEE Applied Power Electronics Conf. and Exposition APEC '04*, vol. 3, 2004, pp. 1389–1394.
- [3] L. Brush, "Distributed power architecture demand characteristics," vol. 1, 2004, pp. 342 – 345 Vol.1.
- [4] S. Vesti, P. Alou, J. Oliver, O. Garcia, R. Prieto, and J. Cobos, "Modeling and simulation of a distributed power system for avionic application," in *Energy Conversion Congress and Exposition (ECCE), 2010 IEEE*, 2010, pp. 4421–4427.
- [5] A. Khaligh, "Realization of parasitics in stability of dc–dc converters loaded by constant power loads in advanced multiconverter automotive systems," vol. 55, no. 6, pp. 2295–2305, 2008.
- [6] D. Boroyevich, I. Cvetkovic, D. Dong, R. Burgos, F. Wang, and F. Lee, "Future electronic power distribution systems a contemplative view," in *Proc. 12th Int Optimization of Electrical and Electronic Equipment (OPTIM) Conf*, 2010, pp. 1369–1380.
- [7] B. Choi, J. Kim, B. H. Cho, S. Choi, and C. M. Wildrick, "Designing control loop for dc-to-dc converters loaded with unknown ac dynamics," vol. 49, no. 4, pp. 925–932, 2002.

- [8] B. Choi, B. H. Cho, and S.-S. Hong, "Dynamics and control of dc-to-dc converters driving other converters downstream," vol. 46, no. 10, pp. 1240–1248, 1999.
- [9] C. M. Wildrick, F. C. Lee, B. H. Cho, and B. Choi, "A method of defining the load impedance specification for a stable distributed power system," vol. 10, no. 3, pp. 280–285, 1995.
- [10] P. Li and B. Lehman, "Performance prediction of dc-dc converters with impedances as loads," vol. 19, no. 1, pp. 201–209, 2004.
- [11] —, "Accurate loop gain prediction for dc-dc converter due to the impact of source/input filter," *Power Electronics, IEEE Transactions on*, vol. 20, no. 4, pp. 754 – 761, July 2005.
- [12] B. Choi, D. Kim, D. Lee, S. Choi, and J. Sun, "Analysis of input filter interactions in switching power converters," vol. 22, no. 2, pp. 452–460, 2007.
- [13] T. Suntio, J. Leppaaho, and M. Hankaniemi, "On emi-filter interactions in a regulated converter - stability and load-transient performance," in *Proc. IEEE Energy Conversion Congress and Exposition ECCE 2009*, 2009, pp. 3031–3038.
- [14] R. Middlebrook, "Input filter considerations in design and application of switching regulators," pp. 336–382, 1976.
- [15] P. G. Maranesi, V. Tavazzi, and V. Varoli, "Two-part characterization of pwm voltage regulators at low frequencies," vol. 35, no. 3, pp. 444–450, 1988.
- [16] L. Arnedo, R. Burgos, D. Boroyevich, and F. Wang, "System-level black-box dc-to-dc converter models," in *Proc. Twenty-Fourth Annual IEEE Applied Power Electronics Conf. and Exposition APEC 2009*, 2009, pp. 1476–1481.
- [17] L. Arnedo, D. Boroyevich, R. Burgos, and F. Wang, "Un-terminated frequency response measurements and model order reduction for black-box terminal characterization models," in *Proc. Twenty-Third Annual IEEE Applied Power Electronics Conf. and Exposition APEC 2008*, 2008, pp. 1054–1060.
- [18] V. Valdivia, A. Barrado, A. Laazaro, P. Zumel, C. Raga, and C. Fernandez, "Simple modeling and identification procedures for ” behavioral modeling of power converters based on transient response analysis," vol. 24, no. 12, pp. 2776–2790, 2009.
- [19] T. Suntio and D. Gadoura, "Use of unterminated two-port modeling technique in analysis of input filter interactions in telecom dps systems," in *Telecommunications Energy Conference, 2002. INTELEC. 24th Annual International*, 2002, pp. 560 – 565.
- [20] T. Suntio, K. Kostov, and J. Tepsa, T. Kyyra, "Using input invariance as a method to facilitate system design in dps applications," *Journal of Circuits, Systems, and Computer*, vol. 13, pp. 707–723, 2004.
- [21] C. W. Deisch, "Simple switching control method changes power converter into a current source," in *IEEE Power Electronics Specialists Conference*, 1978.